Nickel and Iron Aluminides: Processing, Properties and Applications, Cincinnati, OH, Oct. 1996 (ctl asm draft.6 2/19/97)

CONF-961017--30

RECENT ADVANCES IN ALLOY DESIGN OF Ni_3Al ALLOYS FOR STRUCTURAL USE

C. T. Liu and E. P. George
Metals and Ceramics Division
Oak Ridge National Laboratory
Oak Ridge, TN 37831

Abstract

This paper provides a comprehensive review of recent advances in research and development of Ni_3Al-based alloys for structural use at elevated temperatures in hostile environments. Recent studies indicate that polycrystalline Ni_3Al is intrinsically quite ductile at ambient temperatures, and its poor tensile ductility and brittle grain-boundary fracture are caused mainly by moisture-induced hydrogen embrittlement when the aluminide is tested in moisture- or hydrogen-containing environments. The tensile ductility of Ni_3Al is improved by alloying with substitutional and interstitial elements. Among these alloying elements, boron is most effective in suppressing environmental embrittlement and enhancing grain-boundary cohesion, resulting in a dramatic increase of tensile ductility at room temperature. Both boron-doped and boron-free Ni_3Al alloys exhibit brittle intergranular fracture and low ductility at intermediate temperatures (300 to 850°C) because of oxygen-induced embrittlement in oxidizing environments. Chromium is found to be most effective in alleviating elevated-temperature embrittlement. Parallel efforts on alloy development using physical metallurgy principles have led to the development of several Ni_3Al alloys for industrial use. The unique properties of these alloys are briefly discussed.

FOR THE PAST TWO DECADES, considerable efforts have been devoted to the study of brittle grain-boundary fracture and alloy design of the nickel aluminide, Ni_3Al, for structural use at elevated temperatures in hostile environments [1-4]. Light-weight Ni_3Al is of technological interest because of its excellent strength and oxidation resistance at elevated temperatures. Single crystals of Ni_3Al are highly ductile, whereas its polycrystals are brittle in tension at ambient temperatures. The brittleness of Ni_3Al originates at its grain boundaries. Contrary to the common experience with conventional materials, Ni_3Al grain boundaries are usually clean and free of impurities, as evidenced by Auger analyses [5,6]. Similar results were observed in other $L1_2$ ordered intermetallics [1-4]. Because of both scientific and technological interest, substantial effort has been focused on the understanding of the intrinsic grain-boundary brittleness in Ni_3Al and other $L1_2$ intermetallics [7]. Only recently it has become clear that binary Ni_3Al is actually quite ductile at room temperature, and its brittle grain-boundary fracture and low ductility are caused mainly by moisture-induced hydrogen embrittlement when the aluminide is tested in ordinary laboratory air [8-13]. A similar environmental effect has been observed in many other intermetallic alloys with the $L1_2$ structure [14].

The structural use of polycrystalline Ni_3Al was hampered by its brittle grain-boundary fracture at ambient and elevated temperatures. In 1979, Aoki and Izumi [15] first reported that the tensile ductility of Ni_3Al polycrystals was substantially improved by doping with boron additions. Then, Liu et al. [5] found that boron has a strong tendency to segregate to Ni_3Al grain boundaries and that the best ductilizing effect can be achieved only in Ni_3Al with hypostoichiometric compositions (≤ 24 at. % Al). These results have stimulated the interest in the study of alloying effects and alloy design of ductile polycrystalline Ni_3Al alloys for structural applications. At present, several Ni_3Al-based alloys with attractive mechanical and metallurgical properties have been developed, and they are now on the market for industrial use.

This paper provides a comprehensive review of research and development of Ni_3Al alloys. Since several review papers on Ni_3Al alloys were published in conference proceedings [10,12,13], this paper will focus mainly on the recent progress, with emphasis on recent studies of environmental

C.T. Liu

DISCLAIMER

embrittlement in Ni_3Al alloys. This paper contains four additional sections: (1) intergranular fracture and ductility improvement at ambient temperatures, (2) oxygen-induced embrittlement and ductility improvement at intermediate temperatures, (3) alloy design of polycrystalline Ni_3Al, and (4) concluding remarks.

Intergranular Fracture and Ductility Improvement at Ambient Temperatures

Ni_3Al, like many other $L1_2$ intermetallics, exhibits brittle grain-boundary fracture with limited tensile ductility at room temperature [5,15]. After extensive studies, it became clear that the brittle intergranular fracture is caused by two major factors: poor grain-boundary cohesion (intrinsic factor) [8], and environmental embrittlement (extrinsic factor) [8-13]. Previous studies suggested that the grain-boundaries in Ni_3Al might be intrinsically brittle. This was based mainly on Auger analyses which showed no appreciable segregation of impurities on fractured grain-boundary facets [5,6]. During the past several years, however, sufficient evidence has evolved to assert that moisture-induced hydrogen is a major cause of brittle grain-boundary fracture when Ni_3Al alloys are tested in ordinary laboratory air [8-13]. It should be noted that both the intrinsic and extrinsic factors are affected by other metallurgical parameters such as alloy stoichiometry, thermomechanical treatments, impurities, and alloy additions [5,12,16].

In 1991, Liu et al. [8,17] made the first attempt to link brittle intergranular fracture with environmental embrittlement in binary Ni_3Si and Ni_3Al. Table I shows the tensile properties of recrystallized polycrystalline Ni_3Al (24% Al) produced by repeated cold forging and 1000°C-annealing of alloy ingots [8]. The binary aluminide showed only 2.6% elongation in air but 7.2% in dry oxygen, an increase in ductility by a factor of about 3. Later, George et al. [9] reported a larger environmental effect in polycrystalline Ni_3Al (23.4%) carefully prepared by recrystallization of cold-worked single-crystal material. This polycrystalline material also showed a tensile ductility of 3% in air. However, as shown in Fig. 1, its tensile ductility increases steadily as the vacuum improves, and it reaches as high as 23% in an ultra-high vacuum of 10^8 Pa. Their work vividly demonstrated the dominant role of environmental effect on tensile ductility of Ni_3Al at room temperature [9,12].

The environmental effect in Ni_3Al, as well as other aluminides, was suggested to be related to a simple chemical reaction [18,19]:

$$2Al + 3H_2O \rightarrow Al_2O_3 + 6H \qquad \text{Eq. 1}$$

In this reaction, aluminum atoms in Ni_3Al react with moisture in air during testing, resulting in the generation of atomic hydrogen that penetrates along grain boundaries and causes brittle intergranular crack propagation and premature failure. A recent study of the chemical reaction of H_2O with $Ni_3(Al,Ti)$ by XPS [20] provides evidence that H_2O absorbs on the specimen surfaces and then dissociates into hydroxyl (OH) and atomic H. In this case, (OH) preferentially attaches to the

Table I. Effect of Boron Additions on Environmental Embrittlement of Ni_3Al (24% Al) Tested at Room Temperature

Strain Rate (s^{-1})	Test Environment	Elongation (%)	Yield Strength (ksi)	Ultimate Tensile Strength (ksi)
		IC-2: Ni-24 at. % Al		
3.3×10^{-3}	Oxygen	7.2	40.5	63.7
3.3×10^{-3}	Air	2.6	40.6	48.3
		IC-19: Ni-24%Al + 100 wt ppm B		
3.3×10^{-3}	Oxygen	39.5	31.4	189.3
3.3×10^{-3}	Air	18.2	31.2	101.4
3.3×10^{-3}	Water	12.6	30.1	75.2
		IC-15: Ni-24%Al + 500 wt ppm B		
3.3×10^{-3}	Oxygen	39.4	41.9	190.8
3.3×10^{-3}	Air	41.2	42.1	182.9
3.3×10^{-5}	Air	39.4	39.1	177.3
3.3×10^{-5}	Water	38.7	41.8	174.0

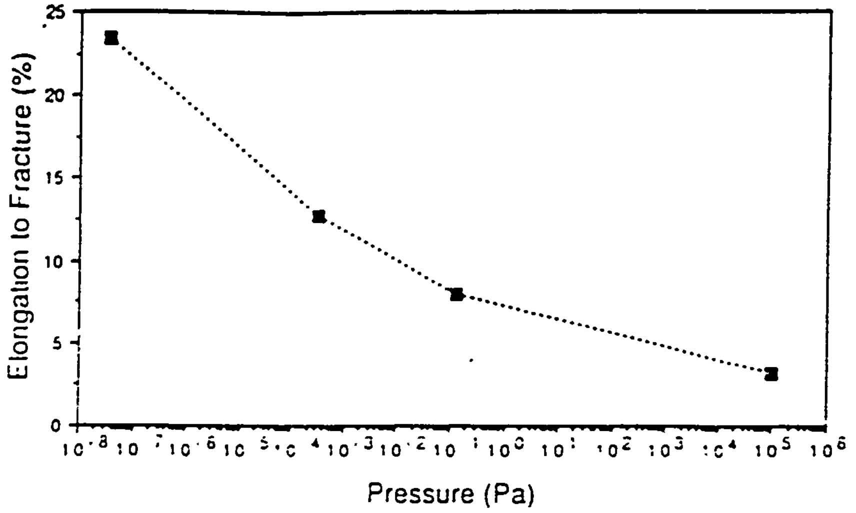

Fig. 1. Room-temperature tensile ductility of polycrystalline Ni-23.4 at. %Al as a function of vacuum level [9].

aluminum atoms and forms Al-OH, whereas atomic H is preferentially associated with nickel atoms. This reaction can be written as:

$$Al + xH_2O \rightarrow Al(OH)_x + xH \qquad \text{Eq. 2}$$

This reaction also generates atomic hydrogen that causes hydrogen-induced embrittlement. Note that H_2O-induced embrittlement is similar to hydrogen embrittlement [21-23], except that hydrogen is generated by the dissociation of moisture in air, rather than from hydrogen sources such as hydrogen gas or cathodically charged hydrogen. Consistent with these reactions, a higher ductility is generally obtained in a vacuum chamber when it is evacuated and back filled with dry oxygen, which suppresses hydrogen generation by direct formation of Al_2O_3. The degree of the embrittlement is affected by two kinetic factors: dissociation kinetics on surfaces and hydrogen diffusion from the surface to bulk. The chemical reaction according to these equations is expected to occur at the places where "fresh" aluminum atoms are available during plastic deformation. Both slip-off steps on surfaces and surface cracks produced during early stages of plastic deformation are possible sites for such chemical reactions to take place. The reaction kinetics suggest reduced hydrogen-induced embrittlement when specimens are strained at high rates. The increase in tensile ductility with increasing testing rate has been observed experimentally [12].

Gleason et al. [24] first reported the possible release of hydrogen from water decomposition on surfaces of polycrystalline aluminides using a temperature-programmed-desorption technique. Recently, Chia and Chung [20] studied the reaction of D_2O molecules with single-crystal $Ni_3(Al,Ti)$ and discovered that the reaction kinetics strongly depend on the crystallographic orientation of the surfaces. Their results indicate that chemically adsorbed D_2O reacts with (100) surfaces and generates deuterium during heating of the specimens to 200°K and above. This confirms the suggested reaction of moisture with aluminides at ambient temperatures. On the other hand, no D_2 was detected during thermal desorption from the (111) surfaces on which D_2O had been chemically adsorbed. These results provide the evidence that the moisture reaction is highly dependent on the atomic arrangement and chemical composition of crystallographic planes. Furthermore, Zhu et al. [25] successfully detected atomic hydrogen produced by the reaction of moisture with an iron aluminide, using laser desorption mass spectrometry. As shown in Fig. 2, H was clearly detected in the FeAl specimens treated with water, while such H was not detected in the specimens treated in vacuum. All these results provide direct support for the proposed reaction that moisture-induced hydrogen is the cause of severe embrittlement in aluminide alloys when tested in moisture-containing environments at ambient temperatures.

Recently, Cohron et al. [26] compared the embrittlement effect of moisture with that of low-pressure H_2 gas in Ni_3Al. Their results are shown in Fig. 3. H_2 at low pressures ($< 10^2$ Pa) does not severely embrittle polycrystalline Ni_3Al (23.4% Al) when the ionization gage (used to measure the vacuum) is turned off, suggesting that molecular H_2 does not dissociate very efficiently into atomic H on Ni_3Al surfaces. On the other hand, low-pressure H_2 is readily dissociated into atomic H by the hot tungsten filament (see Eq. 3) in an ionization gage, which in turn causes severe embrittlement of Ni_3Al. The tensile ductilities measured with the ionization gage on are about half to a quarter of those measured with the gage off. The decrease in the tensile ductilities is accompanied by a change in the fracture mode from ductile transgranular to brittle intergranular. Their results clearly indicate that it is atomic H which causes severe embrittlement, and that the degree of embrittlement is

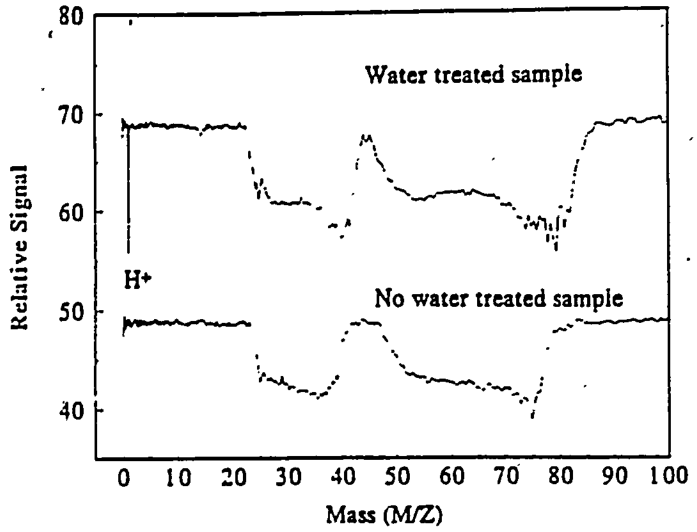

Fig. 2. Measurement of H in vacuum-treated (no water) and water-treated FeAl samples using Laser Desorption Mass Spectrometer [25].

strongly influenced by the kinetics of the dissociation processes from hydrogen-containing molecules into atomic H.

$$H_2 \xrightarrow{\text{hot W filament}} H + H \qquad \text{Eq. 3}$$

Two possible mechanisms are suggested for the penetration of hydrogen from the surface to the interior One is a short-circuit diffusion of hydrogen along grain boundaries, and the other is the transport of hydrogen atoms from specimen surfaces to the grain-boundary region through mobile dislocations generated during plastic deformation [14]. Recently, from the study of environmental embrittlement in $Ni_3(Si,Ti)$, Takasugi et al. [27] found that both prestrain (Fig. 4) and surface blasting substantially reduce the degree of moisture-induced embrittlement at room temperature. If hydrogen atoms were carried to the grain-boundary region mainly by mobile dislocations, we expect that prestrain and surface blasting should promote instead of alleviate environmental embrittlement as shown in Fig. 4. As a matter of fact, the alleviation of environmental embrittlement by prestrain and surface blasting suggests that dislocations trap hydrogen atoms and thus reduce the amount of moisture-induced hydrogen available for grain-boundary penetration and embrittlement. This result also suggests that the grain boundary provides a short-circuit diffusion path for hydrogen penetration.

The tensile ductility of Ni_3Al can be improved by substitutional and interstitial alloying elements [10,28]. Table II lists beneficial elements which improve the tensile ductility of Ni_3Al at room temperature. Among these elements, boron is found to be the most effective in eliminating brittle grain-boundary fracture and increasing the tensile ductility of Ni_3Al with hypostoichiometric compositions ($\leq$24% Al) [5]. This is because boron is able to enhance grain-boundary cohesion and suppress environmental embrittlement. The beneficial effect of boron is also shown in Fig. 5 and Table I. As shown in Fig. 5, unalloyed Ni_3Al containing 24 at. % Al showed brittle grain-boundary fracture with little tensile ductility when tested in air at room temperature. The ductility increased sharply with boron doping and reached more than 40% when doped with > 200 wt ppm B. The increase in ductility was accompanied with a change in fracture mode from brittle intergranular to ductile transgranular. The effect of boron additions on environmental embrittlement is shown in Table I. Ni_3Al (24% Al) doped with 100 wppm B showed a ductility as high as 40% in dry oxygen at room temperature. The ductility, nevertheless, decreased to 18.2% in air and 12.6 % in water, indicating that doping with 100 wppm B is sufficient to take care of the poor grain-boundary cohesion

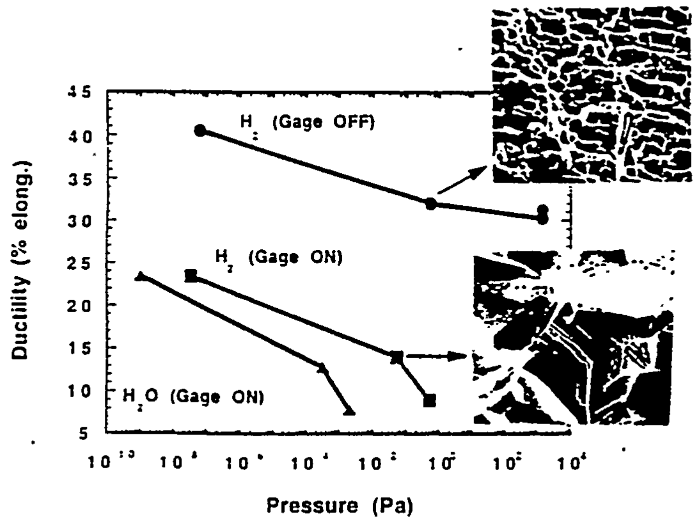

Fig. 3. Effect of test environment (H_2O and H_2) and ion gage (hot filament) on room-temperature ductility of Ni_3Al (23.4 at. % Al) [26].

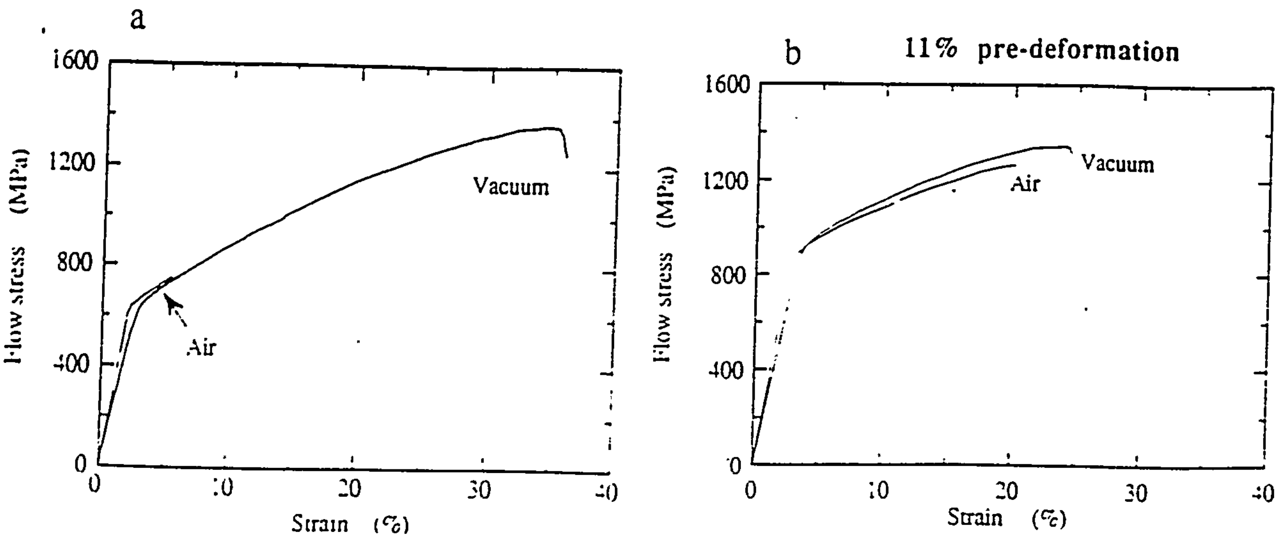

Fig. 4. Effect of prestrain on environmental embrittlement in $Ni_3(Si,Ti)$ polycrystals at room temperature. (a) simply deformed, and (b) prestrained up to 11% in a liquid nitrogen and then strained to fracture [27].

Table II. Effect of Alloying Addition on Room-Temperature Ductility and Fracture Behavior of Ni_3Al Alloys Prepared by Conventional Melting and Casting [28]

Alloying element	Alloy composition (at. %)	Tensile ductile (%)	Fracture mode
	Ni_3Al (24% Al)	1 to 3	Intergranular
B	Ni-24 Al-0.5 B	35 to 54	Transgranular
B. Fe	Ni-20 Al-10 Fe-0.2 B	50	Transgranular
Mn	Ni-16 Al-9 Mn	16	Transgranular
Fe	Ni-10 Al-15 Fe	3	Mixed
Pd	Ni-23 Al-2 Pd	11	Intergranular
Pt	Ni-23 Al-2 Pt	5	Intergranular
Co	Ni-23 Al-2 Co	4	Intergranular
Cu	Ni-23 Al-2 Cu	6	Intergranular
Zr	Ni-22.65Al-0.26 Zr	13	Intergranular

but insufficient to suppress the environmental embrittlement. The aluminide doped with 500 wppm B, on the other hand, showed a high ductility of 40% and transgranular fracture, independent of test environments and strain rates. These results suggest that both poor grain-boundary cohesion and environmental embrittlement have been overcome by doping with as much as 500 wppm B. Auger studies showed that boron tends to segregate to Ni_3Al grain boundaries and that the amount of segregation depends on the bulk concentration of boron [29]. Apparently, boron at levels > 100 wppm is required to suppress moisture-induced hydrogen embrittlement along the grain boundaries. Furthermore, it is found that even more boron doping is necessary in order to ductilize Ni_3Al with near stoichiometric and hyperstoichiometric compositions [28].

Considerable work has been focused on understanding the beneficial effects of boron additions. Both experimental and theoretical studies indicate that boron may provide three beneficial effects: (1) enhancement of grain-boundary cohesion, (2) reduction of hydrogen diffusion along grain boundaries, and (3) reduction of H_2O/Al reaction kinetics. Previous work on atomistic simulation calculations indicated that boron atoms plug atomic-size defects in Ni_3Al grain boundaries and enhance their cohesion [30,31]. Wan et al. [32] demonstrated recently that boron doping reduces hydrogen diffusion along Ni_3Al grain boundaries. In their study, they cathodically charged hydrogen in Ni_3Al doped with 120 and 1000 wppm B. By measuring the depth of the grain-boundary fractured region and correlating it with the mean square penetration depth of hydrogen during cathodic charging, they estimated the grain-boundary diffusivity (D) of hydrogen in two boron-doped materials:

$$\frac{D_{120\ \mathrm{ppm\ B}}}{D_{1000\ \mathrm{ppm\ B}}} = 17 \qquad \text{Eq. 4}$$

This result suggests that boron doping slows down hydrogen diffusion along Ni_3Al grain boundaries and reduces the severity of moisture-induced hydrogen embrittlement.

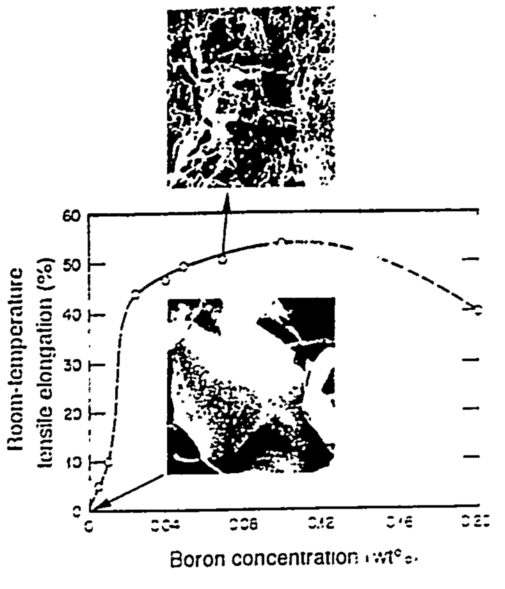

Fig. 5. Effect of boron additions on tensile elongation and fracture behavior of Ni_3Al (24 at. % Al) tested at room temperature.

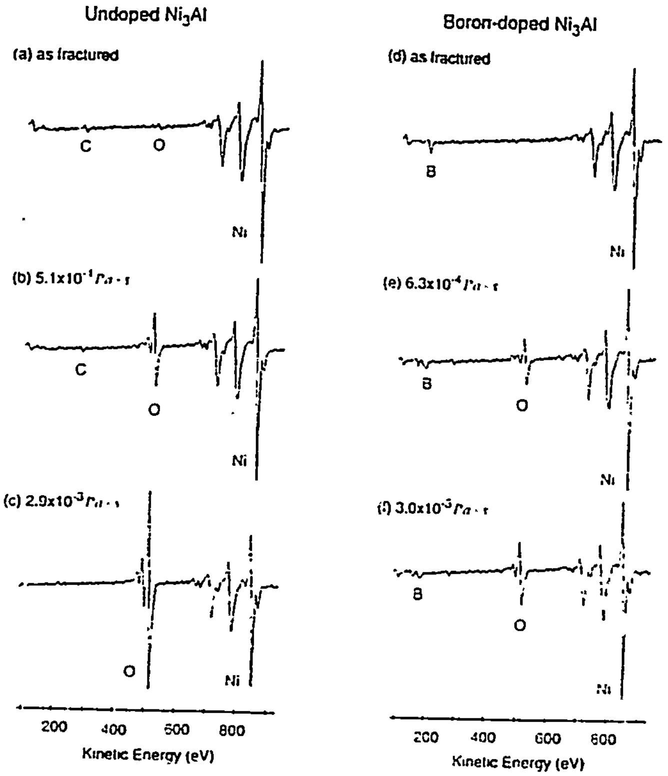

Fig. 6. Auger spectra from intergranular fracture surfaces of undoped (a), (b), (c) and boron-doped (d), (e), (f) Ni_3Al. (a) and (d) as fractured, (b) 5.1×10^{-4}, (c) 2.9×10^{-3}, (e) 6.3×10^{-4}, (f) 3.0×10^{-3} Pa.s exposure. Y axis: EdN (E)/dE, arbitrary scale.

Recently, Lee, Lukowski and White [33] studied the effect of boron segregation on the interaction of water vapor with Ni_3Al grain boundaries. In their study, Ni_3Al specimens with and without boron (650 wppm) were fractured intergranularly in an Auger system. After fracture, water vapor was leaked into the Auger system in order to study the H_2O/Ni_3Al interaction on the fractured surfaces. The comparison of the oxygen peaks shown on the Auger spectra (Fig. 6) obtained from undoped and boron-doped fracture surfaces indicates that boron enrichment (at a level of 8 at. %) on grain-boundaries significantly reduces the kinetics of the surface reaction. This result provides experimental evidence that boron has the beneficial effect of reducing the surface reaction between water vapor and Ni_3Al.

Oxygen-Induced Embrittlement and Ductility Improvement at Intermediate Temperatures

Test environment affects the ductility and fracture of polycrystalline Ni_3Al alloys not only at ambient temperatures but also at elevated temperatures. As mentioned in the previous section, ambient-temperature embrittlement is associated mainly with hydrogen released from the reaction of moisture in air with aluminum atoms in Ni_3Al. The embrittling agent at elevated temperatures is oxygen that penetrates along grain boundaries and causes brittle intergranular fracture [34-37]. Single crystals of Ni_3Al also show a ductility minimum at intermediate temperatures [38], which may also be related to environmental embrittlement.

Recently, George et al. [11] studied the tensile properties as functions of test temperature and environment for polycrystalline binary Ni_3Al (23.4% Al) produced by careful recrystallization of cold worked single-crystal material. Figure 7 is a plot of tensile ductility as a function of test temperature for different test environments. The air-tested curve shows two ductility drops located at around room temperature and 500°C. The low-temperature drop is caused by moisture-induced hydrogen embrittlement, while the higher temperature one is due to oxygen-induced embrittlement.

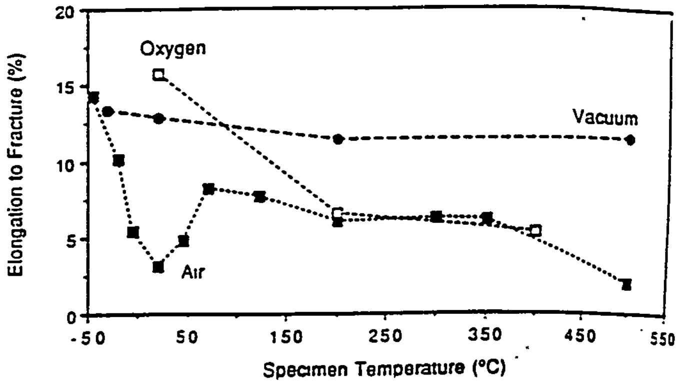

Fig. 7. Effect of temperature on tensile ductility of polycrystalline boron-free Ni_3Al (23.4% Al) in air, vacuum, and oxygen [11].

These two types of embrittlement can be readily understood by comparing the ductility in vacuum with that in air or oxygen. At elevated temperatures, tests in O_2 yield the same low ductilities as those in air, demonstrating that the elevated-temperature embrittlement is due to O_2. Early studies showed that boron-doped Ni_3Al alloys exhibited this elevated-temperature ductility trough [34-37] (see Fig. 8), indicating that boron is not able to suppress O_2-induced embrittlement.

The environment affects not only the tensile properties but also the fatigue behavior. Stoloff et al. reported that the fatigue life of Ni_3Al (24% Al) prepared by powder metallurgy [39] showed a sharp drop in fatigue life above 500°C in a vacuum of 10^{-3} Pa. This result suggests that a conventional vacuum is not good enough to suppress the embrittlement in alloys containing 24% Al. The drop in the fatigue life was accompanied by a change in the fracture mode from transgranular to intergranular.

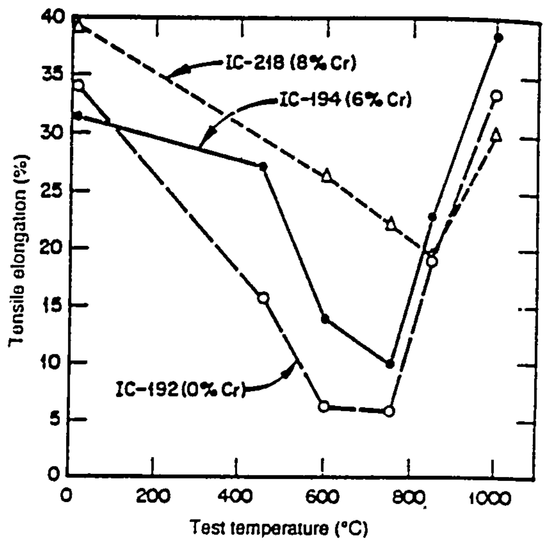

Fig. 8. Effect of chromium additions on the tensile elongation of boron-doped Ni_3Al alloys tested at room temperature to 1000°C [35].

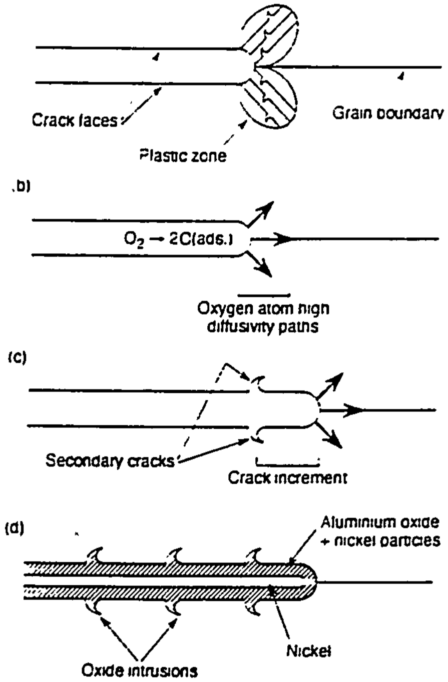

Fig. 9. Schematic illustration of the steps in the proposed fracture mechanism of dynamic embrittlement at elevated temperatures [40].

The embrittlement at elevated temperatures is caused mainly by a dynamic effect involving simultaneously gaseous oxygen, elevated temperature, and localized stress concentration [36]. Such a dynamic effect involves repeatedly weakening and cracking the grain boundaries as a result of oxygen absorption and penetration at crack tips. The reduction in the ductility of Ni_3Al alloys is always accompanied by a change in fracture mode from ductile transgranular to brittle intergranular. Hippsley and DeVan [40] proposed a model of stress-assisted grain boundary oxygen penetration to explain the dynamic embrittlement of Ni_3Al in oxidizing environments at elevated temperatures. This model is similar to the stress-assisted grain boundary oxidation (SAGBO) suggested for oxygen embrittlement [41] in superalloys. According to their model (Fig. 9), the dynamic embrittlement involves the following four sequential steps: (i) occurrence of surface cracks at the initial stage of deformation; (ii) chemisorption of gaseous oxygen to the crack tips where a high localized stress field is involved; (iii) oxygen penetration in its atomic form to the stress field ahead of crack tips; and (iv) inward development of surface cracks preferentially along the grain boundaries, leaving some secondary cracks. Steps (ii) to (iv) proceed continuously and repeatedly during deformation, leading to premature fracture and severe loss in ductility at elevated temperatures.

When Ni_3Al alloys are heat treated extensively in oxidizing environments at elevated temperatures, a penetration of oxygen along grain boundaries may also cause some embrittlement at ambient and elevated temperatures. Takeyama and Liu [42] found that the grain size in Ni_3Al plays an important role in the formation of protective oxide films that affect oxygen penetration along grain boundaries. In their study, Ni_3Al specimens with various grain sizes (17 to 200μm) were preoxidized at 1000°C for 10 min and then tensile tested at 600 and 760°C in vacuum. The results are compared with those from bare specimens tested in vacuum [43] in Fig. 10. The preoxidation causes no embrittlement in the fine-grained, boron-doped Ni_3Al; however, the ductility of the preoxidized specimens decreases with increasing grain size, despite the fact that the ductility of bare specimens is nearly insensitive to the grain size. A severe embrittlement occurs at 760°C for the largest-grained material, with a change in fracture mode from ductile grain boundary fracture for the bare specimen to completely brittle grain boundary fracture for the preoxidized specimen. The loss of ductility is attributed to oxygen penetration along the grain boundary during the preoxidation treatment. Auger analyses revealed a large amount of oxygen on the grain boundaries in the preoxidized, large-grained specimen but little oxygen in the bare specimen. The analyses also revealed an oxygen gradient from the surface to the

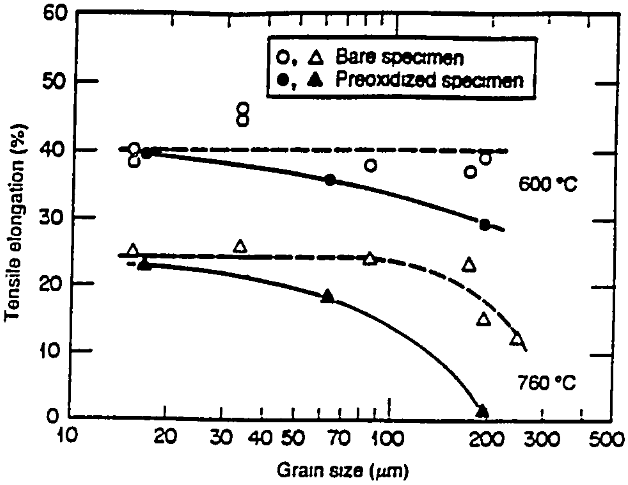

Fig. 10. Change in ductility with grain size of bare and preoxidized Ni_3Al with boron (Ni-23Al-0.5Hf-0.5B, at. %) tested at 600 and 760°C in vacuum [42].

specimen center, indicating a diffusion of oxygen along the grain boundaries in the preoxidized specimen.

The interesting result in the Ni_3Al preoxidation study is the finding that Auger analyses detected no oxygen at the grain boundaries of preoxidized, fine-grained specimens. Such a grain-size dependence of oxygen penetration is related to the difference in the formation of surface oxide films in the fine-grained and large-grained specimens: a continuous, thin, aluminum-rich oxide layer on the specimen surfaces of the fine-grained materials, and a predominantly nickel-rich oxide on the large-grained samples. The former layer effectively blocks oxygen penetration into the alloy and prevents any loss of ductility, whereas the latter allows oxygen to penetrate along the grain boundary and causes severe embrittlement. Formation of aluminum-rich oxide in the fine-grained specimen is a result of short-circuit-path diffusion of aluminum atoms from interior to surface along the grain boundaries.

Oxygen-induced embrittlement is the main cause of the low ductility and brittle fracture in Ni_3Al at elevated temperatures. This problem can be alleviated or reduced by (i) control of surface conditions, (ii) control of grain shape, and (iii) alloy additions. Control of surface conditions is a simple way to alleviate environmental embrittlement resulting from surface reactions. In several cases, preoxidation to form protective oxide scales was proven to be beneficial in reducing oxygen embrittlement at elevated temperatures [36]. Unfortunately, the oxide films crack after a couple of percent strain during tensile testing, and their protective effect disappears. Surface coating with ductile materials should be useful in protecting underlying materials; however, this effect has not yet been well demonstrated. Columnar-grained structures produced by directional solidification have been shown to be effective in reducing environmental embrittlement in Ni_3Al at elevated temperatures [44].

Liu and Sikka [35] reported that chromium is effective in alleviating elevated-temperature embrittlement in oxidizing environments. Figure 8 shows that alloying Ni_3Al with 8 at. % Cr substantially reduced the environmental embrittlement at 600 to 800°C in air. The chromium containing alloys, however, exhibit better ductility in vacuum than in air, indicating that this embrittlement is not completely eliminated by chromium additions. The beneficial effect of chromium is considered to be associated with a rapid formation of self-healing films of chromium oxides that reduce the penetration of oxygen into grain boundaries. The chromium effect is sensitive to alloy composition and microstructure, with the best result from alloys containing 10 to 15 vol. % of the disordered γ phase. We found no other elements which have a beneficial effect on oxygen-induced dynamic embrittlement in Ni_3Al alloys.

Alloy Design of Polycrystalline Ni_3Al Alloys

The mechanical and metallurgical properties of polycrystalline Ni_3Al can be improved by alloying additions. Alloy design efforts have resulted in the development of several Ni_3Al-based alloys with improved properties for structural use [35,45,46]. The compositions of these alloys are listed in Table III. In these aluminide alloys, chromium at a level of 7 to 9 at. % is added for reducing environmental embrittlement in oxidizing environments at elevated temperatures. Zirconium or hafnium additions are most effective in improving the high-temperature strength via solid-solution hardening effects. Molybdenum additions are used for improving strength at ambient and elevated temperatures. Microalloying with boron reduces moisture-induced hydrogen embrittlement and enhances grain-boundary cohesive strength, sharply increasing the ductility at ambient temperatures. Carbides and borides are added to the alloys for additional strengthening effects. In some cases, moderate amounts of cobalt and iron are added to replace Ni, and Al and Ni, respectively, in order to gain further hardness and corrosion resistance. The alloys with optimum properties usually contain 5 to 15 vol. % of the disordered γ phase which has the beneficial effect of reducing environmental embrittlement in oxidizing atmospheres.

Cast aluminide alloys usually possess a coarse grain structure which lowers the yield strength at ambient temperatures. The strength can be increased by alloying with molybdenum via solid-solution hardening [45]. Figure 11 compares the tensile properties of a cast Ni_3Al alloy (IC-221M) with commercial alloys, such as the cast superalloy IN-713C that is commonly used at high temperatures by industry. The strength of the advanced aluminide alloy is comparable to that of IN-713C at room temperature, but it is higher at elevated temperatures because of the significant increase in yield strength with temperature. The aluminide alloys prepared by investment casting showed excellent fatigue resistance. As indicated in Fig. 12, the 650°C high-cycle fatigue life of IC-221M is higher than that of IN-713C by more than two orders of magnitude [47]. The cast aluminide alloys usually have tensile elongations of 10 to 30% at room and elevated temperatures.

Table III. Compositions of Ni_3Al-Base Alloys Available Commercially

Alloy No.	Composition (wt %)	Remarks
IC-50	Ni-11.3Al -0.6Zr-.0.2 B	Fabricable
IC-218	Ni -8.7Al-8.1Cr -0.2Zr-0.02 B	Fabricable
IC-221M	Ni -8.0Al-7.7Cr-1.4Mo-1.7Zr-0.008B	Cast
MX-246*	Ni -8.5Al-7.8Cr-0.9Ti -1.7Zr-0.10B-0.5Mn-0.1C	Fabricable

* From ref. 41.

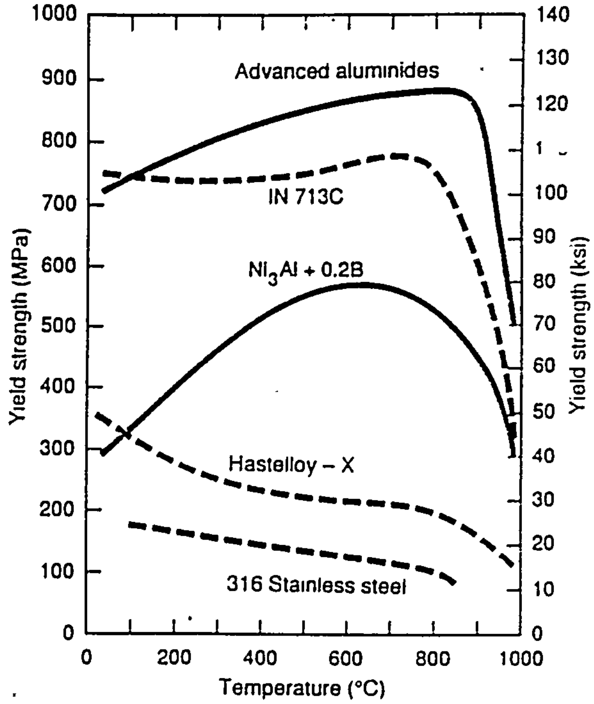

Fig. 11. Comparison of the yield strength of Ni_3Al alloys with that of commercial alloys (IN 713C, Hastelloy X, and type 316 stainless steel) [28].

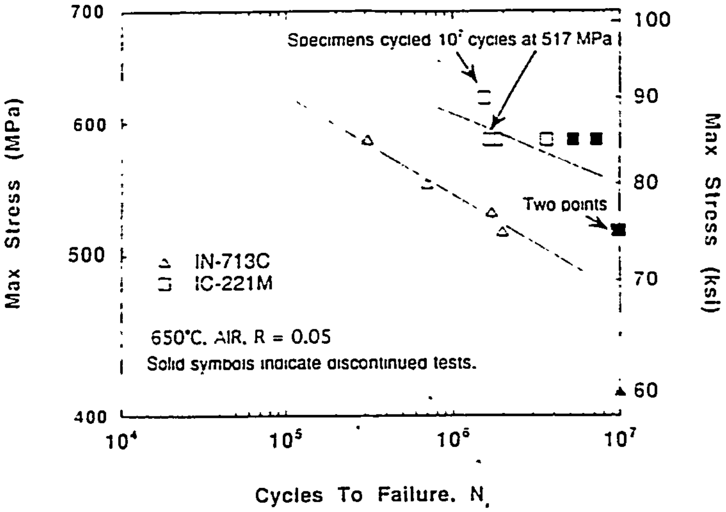

Fig. 12. Comparison of cyclic fatigue life of Ni_3Al-based alloy IC-211M with IN 713C superalloy [47].

The wrought aluminide alloys such as IC-218 can be fabricated by cold rolling or hot extrusion. These alloys are generally not easy to fabricate by hot rolling. Figure 13 shows the stress strain curves of MX246 tested at temperatures to 950°C [46]. This alloy has excellent strength at room temperature ($\sigma_y > 600$ MPa), and its strength increases with temperature and reaches a maximum around 850°C. The alloy showed the lowest tensile ductility around 750°C. The low ductility is due to oxygen-induced embrittlement, as described in the previous section. Because of fine grain structures, the wrought alloys generally showed lower creep resistance, as compared to cast Ni_3Al alloys with coarse grain structures [48]. The wrought and cast alloys generally showed good fatigue crack growth resistance [49]. The fatigue and crack growth behaviors of Ni_3Al alloys are sensitive to the test environment; nevertheless, the aluminide alloys containing chromiumshow fatigue-crack resistance better than chromium-free alloys when tested in air at elevated temperatures [49].

The Ni_3Al alloys exhibit excellent oxidation and carburization resistance at elevated temperatures [50]. This is because these alloys are capable of forming aluminum-oxide scales that protect the alloys from further corrosion in hostile environments. For instance, IC-221 M resistance showed no appreciable weight change even after exposure for several hundred hours at 1100°C in air. The aluminide alloys offer excellent carburization resistance as compared to many common furnace fixture materials such as HU, HK, andAlloy 800 alloys (Fig. 14). The excellent resistance to oxidation and carburization allows the use of Ni_3Al-base alloys at high temperatures for furnace fixtures such as heat-treating trays, posts, and guide rolls [46,50].

Johnson et al. [51] recently reported that Ni_3Al alloys showed excellent cavitation-erosion resistance at ambient temperatures. This is indicated in Fig. 15, where the volume

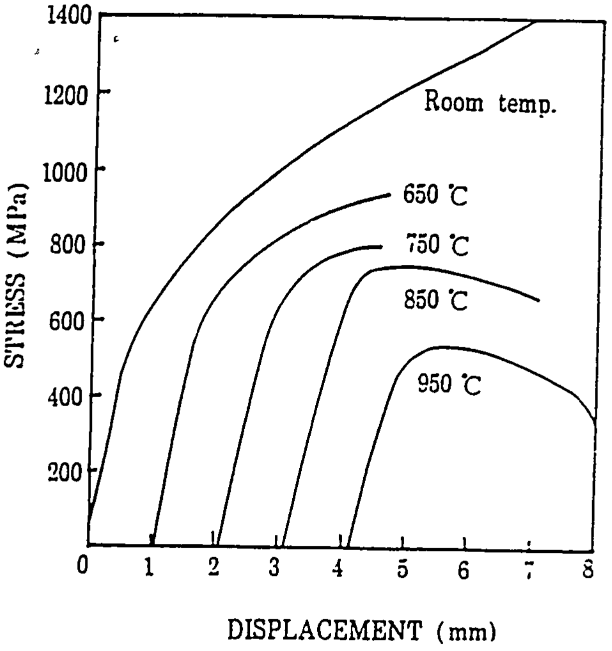

Fig. 13. Stress-strain curves of MX246 (Ni-8.5Al-7.8Cr-1.7Zr-0.9Ti-0.5Mn-0.1C-0.1B, wt %) tested at various temperatures [46].

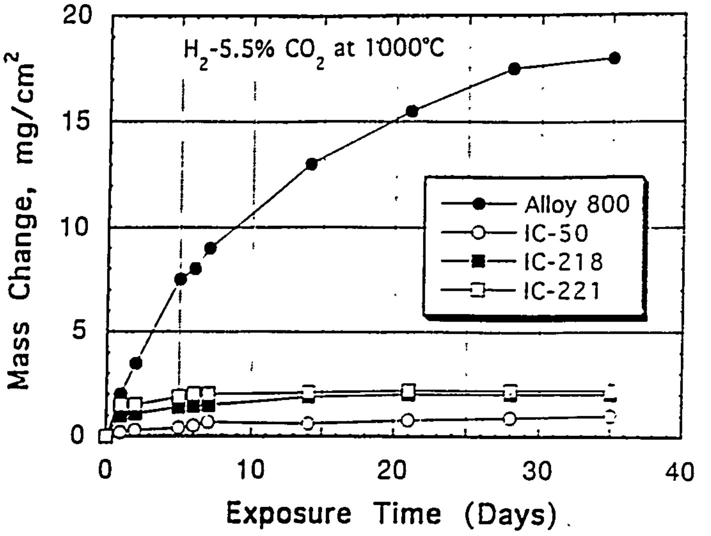

Fig. 14. Comparison of carburization resistance (in H_2-5.5% CO_2) of Ni_3Al-based alloys (IC alloys) with commercialAlloy 800 [50].

loss for different structural alloys is plotted as a function of exposure time for cavitation erosion tests. In comparison with type 316 stainless steel, the rate of cavitation loss of Ni_3Al alloys is lower by a factor of 7. This suggests that Ni_3Al alloys have the potential to be used as coating materials for water turbines in hydroelectric power systems.

Concluding Remarks

Industrial interest in the Ni_3Al alloys developed recently is high at the present time [50,52,53]. This is because the Ni_3Al alloys possess a combination of attractive properties, as listed below, over conventional alloys for structural applications: (1) excellent corrosion resistance in both oxidizing and carburizing environments at elevated temperatures, (2) good strength at temperatures to 1100°C, (3) good fatigue and wear properties at elevated temperatures, (4) low cost for material preparation (take advantage of exothermic reaction and air-casting), (5) excellent resistance to cavitation erosion at ambient temperatures.

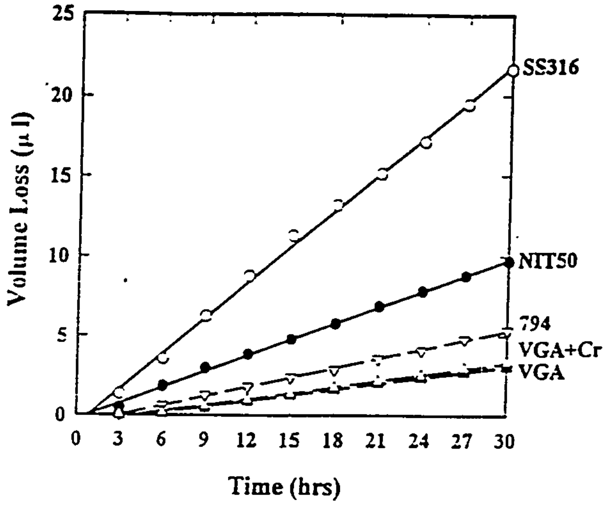

Fig. 15. Comparison of volume loss versus time behavior in cavitation erosion tests for VGA: Ni-25Al (at. %), VGA + Cr: Ni-25Al-8Cr (at. %), 794: Ni-9.5Al-11.2Fe (at. %), NIT 50: Fe-5Mn-1Si-22Cr-12Ni-3Mo-0.3N-0.2Nb-0.2V (at. %). [51].

It should be noted that there are not many structural alloys which have both oxidation and carburization resistance at elevated temperatures. Chromium-base superalloys, for instance, possess good oxidation resistance at temperatures to 1000°C; however, these alloys do not have adequate resistance to carburizing atmospheres because of the easy formation of chromium carbides. A combination of excellent corrosion resistance together with wear resistance and excellent elevated-temperature strength makes Ni_3Al unique for many structural applications. John Orth from United Defense [54] recently reported that the Ni_3Al alloys are excellent materials for tool-and-die applications at ambient and elevated temperatures. During the past year or so, the company has produced nearly 2×10^5 lb of IC-211M for a variety of die and mold applications. Other potential uses of Ni_3Al alloys include transfer rolls to operate at or above 900°C in steel plants, heat-treating trays and posts for operation in carburizing furnaces, rails for walking-beam furnaces, centrifugally cast tubes and static sand-cast return bends for radiant-burner-tube applications in gas-fired heating applications, grate bars used for calcination of ores at high temperatures, hydroturbine, etc. A detailed description of the industrial use of the Ni_3Al alloys is given in the article by V. K. Sikka elsewhere in these proceedings.

In spite of the concentrated effort on Ni_3Al and its alloys, there are areas needing additional research and development. For structural applications, there is room for further property improvement. Suggested future research and development for Ni_3Al alloys include: (i) mechanisms governing the solid-solution hardening behavior at ambient and elevated temperatures, (ii) effect of alloy stoichiometry on moisture-induced hydrogen embrittlement and grain-boundary cohesion, (iii) environmental embrittlement in single-crystal Ni_3Al alloys at elevated temperatures in oxidizing environments, (iv) grain-boundary sliding and superplastic forming, (v) effects of minor additions on creep resistance and hot ductility and fabricability (vi) improvement in hot cracking and weldability of B-doped Ni_3Al alloys, (vii) near-net-shape processing via reaction synthesis, (viii) understanding of solidification processing and cavity formation in cast Ni_3Al alloys, (ix) development of strong single-crystal and directionally solidified Ni_3Al alloys for aerospace applications.

At present, there is world-wide interest in research and development of ordered intermetallic alloys for structural use at elevated temperatures in hostile environments. The knowledge and experience gained from the Ni_3Al studies have been extended to other aluminides, silicides and other intermetallics. A prominent example is the improvement in ductility of Ni_3Al alloys by boron additions [5,15], which was found to have a similar beneficial effect in iron aluminides and other intermetallics [7,55,56].

Acknowledgment

This research was sponsored by the Division of Materials Sciences, U.S. Department of Energy under contract number DE-AC05-96OR22464 with Lockheed Martin Energy Research Corp. Thanks go to Connie Dowker for manuscript preparation.

References

1. MRS Proceedings, "High-Temperature Ordered Intermetallic Alloys," Vol. 39, 81, 133, 213, 288, and 364, MRS Publications, Pittsburgh, PA, 1985 to 1995.
2. S. H. Whang, C. T. Liu, D. P. Pope, and J. O. Stiegler, ed. "High Temperature Aluminides and Intermetallics," Proc. TMS/ASM Symp. (TMS, Warrendale, PA, 1990).
3. S. H. Whang, C. T. Liu, D. P. Pope, and J. O. Stiegler, ed. "High-Temperature Aluminides Intermetallics," *Mater. Sci. Eng.* **A152/A153** (1992).
4. D. P. Pope, C. T. Liu, and S. H. Whang, "High-Temperature Intermetallics," *Mater. Sci. Eng.* **A192/193** (1995).
5. C. T. Liu, C. L. White, and J. A. Horton, *Acta Metall.* **33**, 213 (1985).
6. T. Takasugi, E. P. George, D. P. Pope, and O. Izumi, *Scr. Metall.* **19**, 551 (1985).
7. C. T. Liu, ed. "Intergranular Fracture and Boron Effects in Ni_3Al and Other Intermetallics, a Viewpoint Set in *Scr. Metall.* **25**, 1231-1288 (1991).
8. C. T. Liu, *Scr. Metall.* **27**, 25 (1992).
9. E. P. George, C. T. Liu, and D. P. Pope, *Scr. Metall.* **28**, 857 (1993).
10. C. T. Liu, "Structural Intermetallics," ed. Darolia et al., TMS publications, Pittsburgh, 365-79 (1993).
11. E. P. George, C. T. Liu, and D. P. Pope, *Acta Metall.* **44**, 1757-63 (1996).
12. E. P. George, C. T. Liu, H. Lin, D. P. Pope, *Mater. Sci. Eng.* **A192/193**, 1757-63 (1996).
13. E. P. George and C. T. Liu, MRS Proc. **304**, "High Temperature Ordered Intermetallics," ed. Horton et al., MRS publications, Pittsburgh, 1131-47 (1995).
14. N. S. Stoloff and C. T. Liu, *Intermetallics* **2**, 75-87 (1994).
15. K. Aoki and O. Izumi, *Nippon Kinzoku Gakkaishi* **43**, 1190 (1979).
16. H. Lin and D. P. Pope, *Acta. Metall.* **41**, 553, (1993).
17. C. T. Liu and W. C. Oliver, *Scr. Metall.* **25**, 1993 (1991).
18. C. T. Liu, E. H. Lee, and C. G. McKamey, *Scr. Metall.* **23**, 875 (1989).
19. C. T. Liu, C. G. McKamey, and E. H. Lee, *Scr. Metall.* **24**, 385-90 (1990).
20. W. J. Chia and Y. W. Chung, *Intermetallics* **3**, 505 (1995).
21. A. K. Kuruvilla and N. S. Stoloff, *Scr. Metall.* **19**, 83 (1985).
22. N. S. Stoloff, *J. Metals* **40**, 18 (1988).
23. T. Takasugi, N. Masahashi, and O. Izumi. *Scr. Metall.* **20**, 1317 (1986).
24. N. R. Gleason, C. A. Gerken, and D. R. Strongin, *Appl. Surf. Sci.* **72**, 215 (1993).
25. Y. F. Zhu, C. T. Liu, and C. H. Chen, *Scr. Metall.* **35**, 1435-39 (1996).
26. J. W. Cohron, E. P. George, L. Heatherly, C. T. Liu, and R. H. Zee, *Intermetallics* 4, 497-502 (1996).
27. T. Takasugi, *Intermetallics* 4, 5181-187 (1996).
28. C. T. Liu and D. P. Pope, "Intermetallic Compounds: Principles and Practices," ed. Westbrook and Fleischer, John Wiley and Sons (1994).
29. A. Choudhury, "The Intergranular Segregation of Boron in Substoichiometric Ni_3Al," ORNL/TM-10508, Oak Ridge National Laboratory, Oak Ridge, TN, 37831, Dec. 1987.
30. S. P. Chen, A. F. Voter, R. C. Alberts, A. M. Borong, and J. P. Hay, *Scr. Metall.* **23**, 217 (1989).
31. V. Vitek and S. P. Chen, *Scr. Metall.* **25**, 1237-42 (1991).
32. X. J. Wan, J. H. Zhu, K. L. Jing, and C. T. Liu, *Scr. Metall.* **31**, (1994).
33. K. H. Lee, J. T. Lukowski, and C. L. White, *Scr. Metall.* **35**, 1153-59 (1996).
34. C. T. Liu, C. L. White, and E. H. Lee, *Scr. Metall.* **19**, 1247-1250 (1985).
35. C. T. Liu and V. K. Sikka, *J. Metal* **38**, 19 (1986).
36. C. T. Liu and C. L. White, *Acta Metall.* **35**, 643 (1987).
37. A. I. Taub, K.-M. Chang, and C. T. Liu, *Scr. Metall.* **20**, 1613 (1986).
38. P. H. Thornton, R. G. Davies, and T. L. Johnston, *Metall. Trans.* **1**, 207 (1970).
39. N. S. Stoloff, G. E. Fuchs, A. K. Kuruvilla, and S. J. Choe, p. 247 in ref. 2(1987).

C.T. Liu

40. C. A. Hippsley and J. H. DeVan, *Acta Metall.* **37**, 1485 (1989).
41. H. W. Carpenter, *Met. Prog.* **110**, 25 ( ).
42. M. Takeyama and C. T. Liu, *Acta Metall.* **37**, 2681 (1989).
43. M. Takeyama and C. T. Liu, *Acta Metall.* **36**, 1241 (1988).
44. C. T. Liu and B. F. Oliver, *J. Mater. Res.* **4**, 294 (1989).
45. C. T. Liu, U.S. Patent **5**, 108,700 (1992).
46. Feng Di, Ye Nujun, Han Guangwei, and Luo Heli, *Acta Metall. Sinica* **8**, 503 (1995).
47. B. G. Gieseke and V. K. Sikka, unpublished results, Oak Ridge National Laboratory, Oak Ridge, TN 37831 (1992).
48. V. K. Sikka, *Mater. Manuf. Proc.* **4**, 1-24, (1989).
49. W. Matuszyk, G. Camus, D. J. Duquette, and N. S. Stoloff, *Metall. Trans.* **21A**, 2967 (1990).
50. S. C. Deevi and V. K. Sikka, *Intermetallics* **4**, 357 (1996).
51. M. L. Johnson, D. E. Mikkola, and Wright, *Intermetallics* **3**, 389-96 (1995).
52. S. C. Deevi and V. K. Sikka, *Intermetallics* **4** (in press) (1996).
53. V. K. Sikka, J. T. Mavity, and K. Anderson, *Mat. Sci. Eng.* **A153**, 712 (1992).
54. J. Orth, paper presented at the DOE Workshop on Intermetallic Alloys held in Atlanta, Georgia, June 3-4, 1996.
55. C. T. Liu and E. P. George, *Scr. Metall.* **24**, 1285-90 (1990).
56. P. J. Maziasz, G. M. Goodwin, C.T. Liu, and S.A. David, *Scr. Metall.* **27**, 1835 (1992).